CHEMISTRY OF MATERIALS

Article

pubs.acs.org/cm

Transformation Mechanism of Magnesium and Aluminum Precursor Solution into Crystallites of Layered Double Hydroxide

Yanmin Yang, Xiaofei Zhao, Yue Zhu, and Fazhi Zhang*

State Key Laboratory of Chemical Resource Engineering, Beijing University of Chemical Technology, Beijing 100029, China

Supporting Information

ABSTRACT: Layered double hydroxides (LDHs), members of a family of two-dimensional anionic clay with flexibility in composition, have found a wide variety of applications in industry, including as additives in polymers, as precursors to magnetic materials, in biology and medicine, in catalysis, and in environmental remediation. A detailed understanding of the mechanism of the LDH formation should gain deep insight on the synthetic methodologies of the material and further allow the properties of the resulting LDH to be tailored to specific applications. Herein, we report a systematic investigation of the formation mechanism of the typical MgAl-LDH by urea precipitation method from a magnesium and aluminum precursor salt solution. It is revealed that, at the first stage of the synthesis, amorphous colloidal hydroxide aluminum is formed from the aluminum precursor salt solution. Then, the amorphous hydroxides are transformed into the crystallites of oxide-hydroxide aluminum boehmite γ-AlOOH, accompanying the continuous incorporation of surrounding Mg^{2+} into the sheet of the lamellar γ-AlOOH, leading to the charge imbalance of the sheet, which destroys the hydrogen bonds existing between the sheets. Subsequently, the carbonate ions in the solution are intercalated into the interlayer galleries by an electrostatic interaction for balancing the sheet charge, resulting in an initial LDH phase with alveolate-like structure. Finally, the main layers stack to build a three-dimensional network with the positive charge being balanced by the carbonate ions arranged in the hydrated interlayer galleries, and the integrated plate-like structure of LDH is formed. Throughout the above-mentioned processes, the incorporation of magnesium ions into the sheet of the lamellar boehmite can play a primary role for the formation of LDH crystallites.

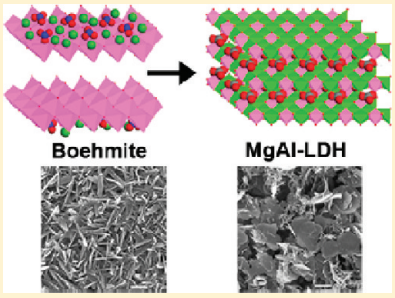

KEYWORDS: *layered double hydroxides, hydrotalcite, formation mechanism, nucleation, HRTEM, lamellar*

INTRODUCTION

Layered double hydroxides (LDHs), also known as hydrotalcite-like compounds, are a class of layered materials with the general chemical composition $[M^{2+}_{1-x}M^{3+}_{x}(OH)_2](A^{n-})_{x/n}\cdot mH_2O$, where M^{2+} and M^{3+} are di- and trivalent cations, respectively, A^{n-} is an interlayer anion with charge n, and x is the $[M^{3+}]/([M^{2+}] + [M^{3+}])$ molar fraction.[1] The structure of LDHs is best understood by considering brucite, $Mg(OH)_2$, which consists of infinite sheets of edge-sharing MgO_6 octahedra. If the divalent cations are partially substituted by the trivalent cations, the sheets will have a positive charge. Simultaneously, appropriate numbers of anions reside in the hydrated interlayer galleries to balance the positive charge.[2] A major advantage of LDHs as functional materials or their precursors is that their composition is very flexible: the identity of the di- and trivalent metal ions, their atomic ratio, and the nature of the interlayer anion can be varied over a wide range without altering the basic structure of the material. As a result, LDHs are excellent anion clay materials and find application in diverse areas such as catalysts or catalyst precursors, anion exchangers, flame retardants, stabilizers for polymers, and electroactive and photoactive materials, as well as in the medical field as antacids and for controlled release.[3]

An increasing growth of research efforts have been made to realize systematic control over the structure and morphology of inorganic nanocrystals, owing to their potential and promising applications in a variety of fields.[4] As a layered material, LDH crystallites tend to have a smooth platelet morphology, in which the dimensions of the (typically hexagonal) basal crystal faces of the platelets are much larger than the thickness (the lateral crystal faces) of the platelets. Hitherto, various synthesis strategies and techniques associated with control of particle size, structure, morphology, crystallinity, and orientation of the resulting LDH have been developed. For example, the well-crystallized LDH crystals with large platelets in micrometer sizes could be obtained by urea or hexamethylenetetramine hydrolysis in homogeneous precipitation reactions.[5] A modified coprecipitation method for stable homogeneous LDH suspensions with controllable particle sizes has been reported, which involved a fast coprecipitation of mixed salt solutions and alkali solutions at room temperature and ambient pressure followed by hydrothermal post-treatment under controlled temperature and time.[6] A narrower particle size distribution for LDH nanomaterial could be prepared by a discontinuous method, through a rapid mixing and nucleation in a colloid mill followed by a separate aging step, compared with conventional

Received: July 7, 2011
Revised: December 4, 2011
Published: December 19, 2011

   dx.doi.org/10.1021/cm201936b | *Chem. Mater.* 2012, 24, 81–87

coprecipitation at constant pH.[7] An in-line dispersion−precipitation method for the preparation of LDH materials with tunable properties was reported.[8] This was accomplished by performing the precipitation in continuous mode using a vigorously stirred microreactor with in-line pH control at fixed residence time. Besides, a water-in-oil reverse microemulsion system has been applied in the LDH synthesis with unique morphologies.[9] The adopted system is the reverse microemusion of sodium docecylsulfate−water isooctane with water/surfactant molar ratio of 24. Additionally, the effects of some synthesis parameters on the LDH crystallinity have been investigated. For example, the influence of the pH values in the course of synthesis on the properties of MgAl-LDH by coprecipitation was already discussed.[10] It was shown that the best result for obtaining LDH of a given cationic composition was at pH values ranging from 10 to 13.2.

Despite the above-mentioned achievements made for the controllable preparation of LDH, few reports had been focused on the formation mechanism of the material.[10,11] According to the literature, a rough two-stage formation process was commonly proposed for the synthesis of MgAl-LDH by coprecipitation:[10,11b−d] the first stage corresponds to the formation of aluminum hydroxide or hydrous oxide in the presence of excess Al^{3+}, followed by the formation of LDH from aluminum hydr(ous)oxide in the presence of excess Mg^{2+}. Nevertheless, at the second stage, the crystallization of LDH occurring by means of the diffusing of aluminum atoms into the magnesium hydroxide structure[11c] or through the incorporation of magnesium continuously into an Al-rich LDH-type phase[10,11b,d] has not been thoroughly revealed at present. In spite of these efforts to understand the LDH evolution process, research has not been able to gain adequate and direct information to clearly reveal the formation process, such as the evolution of particle morphology, phase composition, and structure during the whole process.

In this work, we report a systematic investigation of the formation mechanism of MgAl-LDH in carbonate form, which is the most commonly studied hydrotalcite-like material, by using high resolution transmission electron microscopy (HRTEM) combined with selected area electron diffraction (SAED), field emission scanning electron microscopy (FESEM), X-ray diffraction (XRD), Fourier transform infrared (FT-IR), X-ray photoelectron spectroscopy (XPS), and inductively coupled plasma emission spectrometry (ICP-ES) measurements. For the purpose of monitoring the whole process of LDH formation, especially gaining the more detailed information about the early stage of the reaction, MgAl-LDH was synthesized by urea precipitation method from homogeneous solution using the temperature-controlled hydrolysis of urea, which gives the required gradual increases in both pH and concentration of carbonate ions.[5c] The mechanism of LDH formation is discussed based on the characterization results of specimens. We hope that our detailed understanding of the nucleation and growth of LDH crystallites will be of considerable importance for gaining deep insight on the synthetic methodologies of the material and will further allow the properties of the resulting LDH to be tailored to specific applications.

EXPERIMENTAL SECTION

Preparation of MgAl-LDH (Experiment I). The synthetic method for MgAl-LDH was used as previously described by Costantino and co-workers.[5c] To slow the nucleation rate to gain more detailed information about the early stage of the reaction, the method with changed parameters, such as reaction time, metal salt concentrations, urea amount, and the final ratio of urea/(M^{2+}+M^{3+}) were employed. All reagents were analytical grade without further purification. The melt salt was prepared by mixing 29.9 g of magnesium nitrate hexahydrate and 21.9 g of aluminum nitrate nonahydrate with 100 mL of deionized water, followed by dissolving 27.3 g of urea into 100 mL of deionized water in another beaker. The two solutions were put into a supersonic cleaner until they all became clear, and then they were added into a three-neck flask under continuous stirring and refluxing. An additional 150 mL of deionized water was also added simultaneously. The flask was soaked in a water bath previously heated to 90 °C. The final concentrations of the melt salt were [Mg^{2+} + Al^{3+}] = 0.5 mol/L, Mg^{2+}/Al^{3+} = 2.0, and urea/[Mg^{2+} + Al^{3+}] = 2.5 in the solution that was used. The initial reaction time was recorded as 0 h when the mixed solution became turbid. Afterward, the reaction was stopped at different times. The final specimens were designated as LDH(x), where x stands for reaction time in hours after the solution became turbid. The samples were washed repeatedly with anhydrous ethyl alcohol, followed by freeze preservation in a refrigerator.

Preparation of MgAl-LDH by Adding a Magnesium Precursor (Experiment II). The experiment was first conducted by stirring 400 mL of a mixed solution of aluminum nitrate nonahydrate (ca. 31.3 g) and urea (ca. 37.5 g) at 90 °C. The initial reaction time was recorded as 0 h when the mixed solution became turbid, after about 6.5 h. Samples (50 mL) were taken at different reaction times: 0 h, 4 h, 8 h, 24 h, and 48 h (designated as AU(x), where x stands for reaction time in hours). The supernatant of the first-time centrifugal AU(48) sample was collected for further ICP detection. After the reaction time of 48 h, 150 mL of a solution of magnesium nitrate hexahydrate (ca. 12.8 g) was added. The concentration ratio of urea/Al/Mg was approximately the same as in experiment I. Then, samples were taken after reaction times of 16 h, 24 h, 48 h, and 72 h (designated as AU-M(16), AU-M(24), AU-M(48), and AU-M(72), respectively), with a capacity of 50 mL. All samples were washed several times with deionized water and anhydrous ethyl alcohol and dried in an oven at 90 °C overnight.

Characterization. XRD patterns of the prepared samples were recorded on a Shimadzu XRD-6000 power diffractometer using Cu Kα radiation (λ = 1.5418 Å) at 40 kV and 30 mA in the 2θ range of 3−70° with a scanning rate of 0.2°/min. FT-IR spectra of samples were collected in KBr pellets on a Bruker Vector-22 Fourier transformation infrared spectroscope in reflectance mode, at the range of 400−4000 cm^{-1}, with a resolution of 2 cm^{-1}. Elemental analysis of the samples was performed using a Shimadzu ICPs-7500 inductively coupled plasma emission spectrometer. The samples for ICP were prepared by dissolving the as-prepared products in dilute hydrochloric acid (1:1) at room temperature. The C, H, and N contents were determined using a varioEL cube V2.0.1 elemental analyzer. The morphology of the samples was analyzed by FESEM, using a JEOL JSM-7001F microscope equipped with a GENESIS III energy dispersive X-ray (EDX) spectrometer operating at 20.0 kV. The composition data obtained by EDX analyses referred to metal atoms only; all other atoms were omitted. A software program automatically processed the signals from the backscattered electron detector. The samples for FESEM were prepared by suspension of the powders in ethanol and ultrasonication for 0.5 h. A drop of the resulting suspension was dropped onto the single-crystal silicon wafer and then coated with Au to act as conductive film in order to reducing the beam charging. TEM and HRTEM images and SAED patterns were obtained on a JEOL JEM-2100 transmission electron microscope, operating at an accelerating voltage of 200.0 kV. The samples for TEM were prepared as follows: the powders with different reaction times were suspended in ethanol and ultrasonicated for 0.5 h. A drop of the resulting suspension was then deposited onto the TEM sample stage coated with commercially available amorphous holey-film carbon-coated copper grid. XPS measurements were recorded on an ESCALAB 250 X-ray photoelectron spectrometer, operating at a typical pressure

dx.doi.org/10.1021/cm201936b | Chem. Mater. 2012, 24, 81−87

of about 2 × 10^{-9} Pa using Al Kα X-rays as the excitation source (1486.6 kV) in 0.05 eV energy step size.

RESULTS AND DISCUSSION

MgAl-LDH was synthesized by urea precipitation method from homogeneous solution using the temperature-controlled hydrolysis of urea. When the reaction solution turned into a transparent milk-white colloidal after the addition of the magnesium and aluminum precursor salt solution into a three-neck flask for 4.5 h, the reaction time was recorded as 0 h. The long time for the first precipitation is because the thermal activation of urea decomposition at ambient pressure requires a long reaction time.[12] The XRD patterns of the specimens after different reaction times are shown in Figure 1. The diffraction

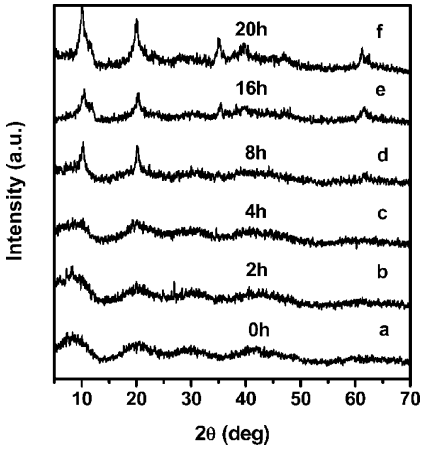

Figure 1. XRD patterns of MgAl-LDH samples prepared with different reaction times.

pattern of LDH(0) (Figure 1a) displays broad peaks centered at 2θ positions characteristic of amorphous pseudoboehmite aluminum hydroxide gel.[13] When the reaction time was extended beyond 8 h, weak diffraction peaks characteristic of LDH begin to appear, as seen in Figure 1d.[14] When the hydrothermal treatment was increased from 8 to 20 h, the diffraction peaks of LDH gradually become sharper, indicating that the crystallinity of LDH increases with increasing reaction time. It is thought that better resolved diffraction lines of the LDH will appear when the reaction time is extended beyond 20 h.

The morphologies of the resulting samples were examined by SEM and TEM techniques. The SEM images of LDH(0) and LDH(2) show the agglomerates of amorphous gel particles with multifarious shapes as well (Figure 2a and b), which is in good agreement with the XRD results (Figure 1a and b). After hydrothermal treatment for another 2 h, it is interesting to see in Figure 2c that alveolate-like particles appear in LDH(4), which is not revealed in the LDH crystallization process by previous reports. More SEM images of LDH(4) sample particles are given in Figure S1 in the Supporting Information. It can be seen that all the particles have the rounded alveolate-like structure. The high magnification SEM image of LDH(4) shows that numerous nanoflakes curve from the surface of the particle (Figure 2c′). When the duration of reaction was further prolonged, a large number of particles with plate-like morphology appear in the SEM images, which are characteristics of plate-like LDH crystalline (Figure 2d, e, and f). Besides, the particle size increases gradually with the reaction time.

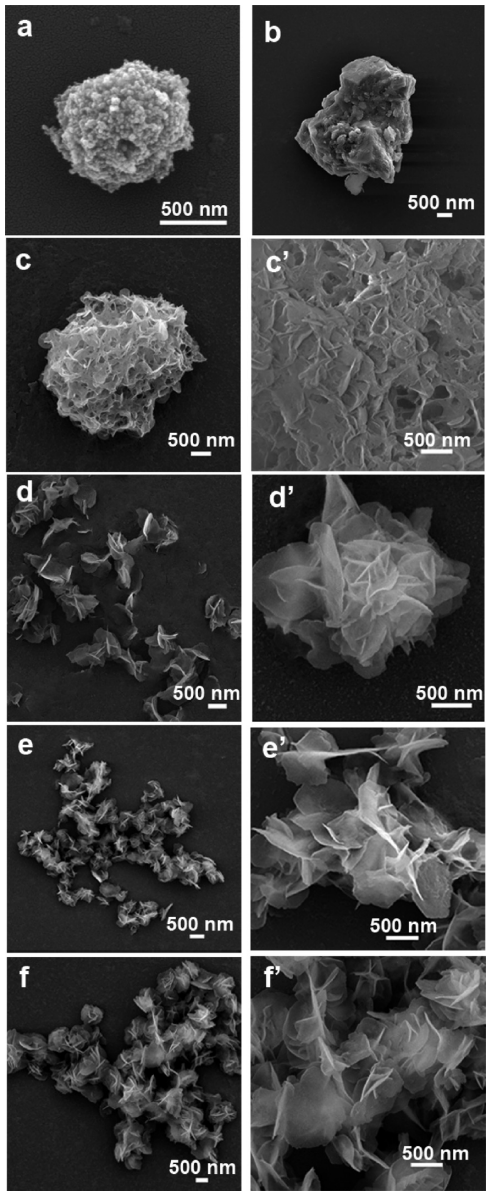

Figure 2. SEM images of MgAl-LDH samples with different reaction times: (a) 0 h, (b) 2 h, (c) 4 h, (d) 8 h, (e) 16 h, (f) 20 h. High magnification SEM images of the samples: (c′), (d′), (e′), and (f′), respectively.

These results coincide with those of the XRD patterns, which show the diffraction peaks of LDH for the samples with hydrothermal treatment times longer than 8 h, and the crystallinity of LDH increases with increasing reaction time. It can be clearly seen from the high magnification images (Figure 2d′,e′, and f′) that the plate-like LDH is ultrathin and curled, which is attributed to the small molar ratio of urea/[Mg^{2+}+Al^{3+}] and short crystallization time employed. The EDX and ICP results were both plotted as a function of reaction time, given in Figure 3. It is apparent from the ICP results that, at the early stage of the crystallization, the content of Mg in the specimens is very little. As time goes on, the Mg/Al ratio first increases very slowly and then undergoes a quick rise after the reaction time exceeds 8 h. The same trend is also demonstrated through the EDX curve. The Mg/Al ratio of LDH(4) is about 0.20, but it increases to 1.60 in LDH(72). It is noted that the value of the Mg/Al ratio obtained from the bulk chemical

dx.doi.org/10.1021/cm201936b | Chem. Mater. 2012, 24, 81–87

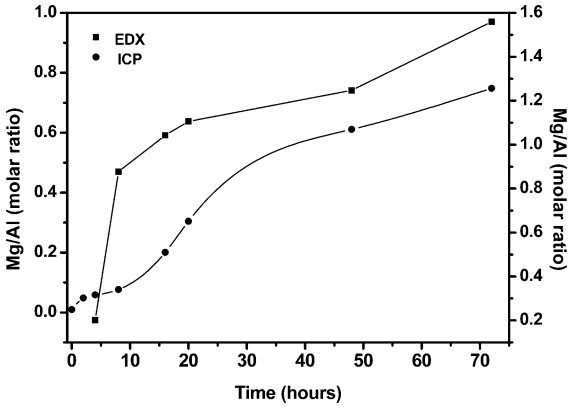

Figure 3. Evolution of the Mg/Al molar ratio, examined by ICP (the left *y*-axis) and EDX (the right *y*-axis), for MgAl-LDH samples prepared with different reaction times.

composition determined by ICP analyses is much lower than that obtained with EDX detection. The reason for this difference is that ICP determination requires all of sample to be transferred into a liquid phase and inspects all of the metal content while EDX detection measures the selected area on a single LDH particle with a sampled depth of approximately 1–3 μm.[15] Moreover, the Mg/Al ratio of the final sample LDH(72) (1.60) is lower than the predicted ratio of 2.0 from the synthesis solution. The urea homogeneous precipitation method is not indicated for the preparation of MgAl-LDH with low charge density, but it allows the preparation of compounds with high charge density, which is not easily obtainable with the other proposed procedures.[5c] This also means that MgAl-LDH with a Mg/Al ratio less than 2.0 (so-called Al-rich LDH) is often obtained by this method. Coupled with the ICP and EDX results, we can conclude that the absorbed Mg^{2+} ions were gradually incorporated into the pseudoboehmite specimen to fabricate LDH, while a quantity of this amorphous aluminum still exists in all samples but with a progressive decrease in content.

TEM images of the LDH(2) and LDH(8) samples are shown in Figure 4. Figure 4a indicates that there is an amorphous phase in the LDH(2) sample, which is in good agreement with the XRD examination (Figure 1b). The particles of LDH(8) possess the plate-like hexagonal crystal habit (Figure 2d). Particles that are oriented perpendicular to the plane of the sample stage for the TEM examination are seen as dark lines (Figure 4d). Meanwhile, the sharp contrasts among the dark lines of these plates and the faded area underneath confirm that there are still amorphous specimens exiting in the LDH(8) sample. Further evidence of the appearance of LDH crystalline phase was given by HRTEM image and the corresponding SAED pattern (Figure 4d). The lattice fringes of (101) planes with a lattice gap of 0.270 nm and an amorphous phase (designated by white arrows) can both be demonstrated (Figure 4d). In addition, periodic diffraction concentric rings verify the polycrystalline nature of the sample by the SAED pattern (inserted in Figure 4d): the two rings can be attributed to the (110) and (2011) crystal planes of LDH, according to JCPDS PDF No. 890460. Also, it is obvious that the lattice fringe and the diffraction spots are relatively weak, as a result of the short crystallization time. It is worth mentioning that numerous tiny nanoparticles are distributed on the whole surface of the samples (Figure 4c). These tiny nanoparticles would be the initial crystal nuclei at the early crystallization stage for the growth of LDH crystalline; the process is then thermodynamically further driven toward crystallization of those tiny nanoparticles with an increase in the reaction time; and thus, the irreversible aggregation of these randomly moving nanoparticles results in the self-clustering growth and formation of LDH hierarchical architectures.

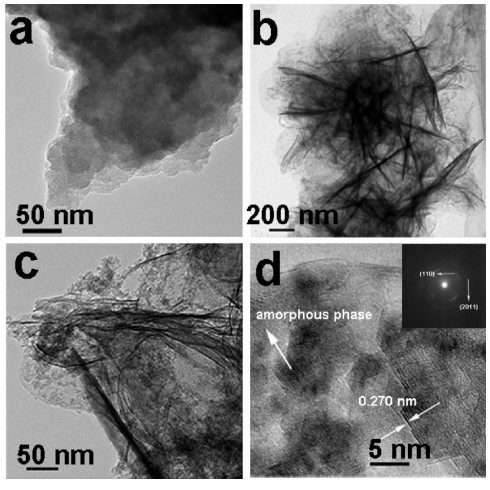

Figure 4. TEM images of MgAl-LDH samples: (a) LDH(2) and (b) LDH(8). (c) High-magnification view of (b). (d) HRTEM image of (b) with an inserted corresponding SAED pattern.

To get better evidence of the LDH formation process, FT-IR, CHN elemental analysis, and XPS investigations were also employed. The FT-IR spectra show that, at the initial crystallization stage (Figure 5a–d), the resulting aluminum hydrous(oxide) contains an intense adsorption band around

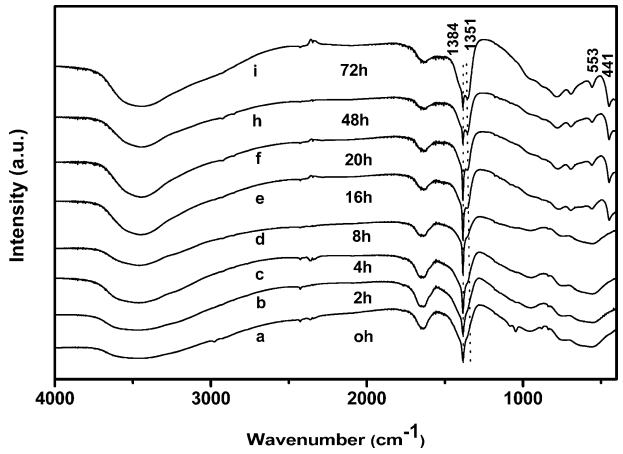

Figure 5. FT-IR spectra of MgAl-LDH samples prepared with different reaction times.

1384 cm^{-1},[16] which is ascribed to the symmetric stretching mode of the nitrate ions. Then, the absorption band of carbonate ions at 1354 m^{-1} appears[16] (Figure 5e–i), verifying that the NO_3^- ions are progressively replaced by the CO_3^{2-} ions. When the reaction time is beyond 20 h, the carbonate absorption band is much more obvious and the intensity of the nitrate ions reduces gradually (Figure 5h and i). The CHN elemental analysis results are 2.682% N, 0.50% C, 4.175% H for LDH(0) and 0.741% N, 1.71% C, 4.423% H for LDH(20). The mass fraction changes between N and C atoms are consistent

dx.doi.org/10.1021/cm201936b | *Chem. Mater.* 2012, 24, 81–87

with the FT-IR results. Furthermore, the total mass fraction of N and C atoms in LDH(0) (3.182%) is much higher than that in LDH(20) (2.451%), which is probably because of the mass absorptive NO_3^- ions on the surface of amorphous aluminum hydroxide.

The XPS spectra of Mg 1s and Al 2p for the MgAl-LDH specimens prepared with different reaction times were given in Figure 6. We can recognize that at the early crystallization stage (specimens prepared with reaction times 0 h, 2 h, and 4 h), the

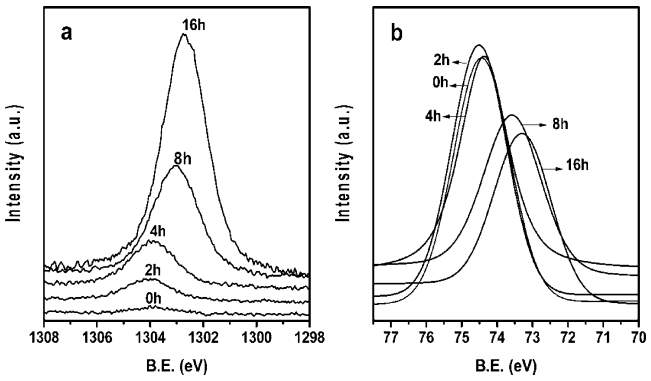

Figure 6. XPS spectra of Mg 1s (a) and Al 2p (b) for MgAl-LDH samples prepared with different reaction times.

binding energies of Mg 1s are approximately in the same region (Figure 6a). At the later stage, the binding energies of the two specimens prepared with reaction times of 16 and 20 h are similar and both shifted to the lower values. The XPS spectra of Al 2p show the same trend (Figure 6b). We conclude that the electronic atmosphere of Mg and Al atoms is changed dramatically when expanding the reaction time from 4 to 8 h, which is caused by the incorporation of Mg^{2+} in the pseudoboehmite aluminum gel. It is revealed that the structure of MgAl-LDH consists of infinite sheets of edge-sharing MgO_6 or AlO_6 octahedra.[1e] Thus, after the Mg^{2+} ions in the reaction solution are incorporated into the sheets forming MgO_6 octahedral, the binding energy can be shifted to lower region as the crystallinity and electron cloud density surrounding the magnesium nuclei increase. Meanwhile, the binding energy of Al 2p is also shifted to lower values for the Mg^{2+} ions that were introduced to the aluminum hydroxide during this period, probably by Mg^{2+} substituting Al^{3+} of the AlO_6 octahedra to destroy the Al−O−Al and reform Al−O−Mg bond, which leads to the reinforcement of the electron cloud density of aluminum nuclei and/or by Mg^{2+} entering the octahedral vacancy, which is caused by the close interaction of adjacent AlO_6 octahedra.[17]

We carried out an additional experiment to further verify the evolution process of LDH formation (experiment II). The experiment was first conducted by stirring the mixed solution of aluminum nitrate nonahydrate and urea for about 6.5 h before the solution became turbid (indexed as 0 h). The XRD patterns of samples taken at different reaction times are shown in Figure 7. An amorphous phase can be identified at the early stage (Figure 7a−c). With the reaction time of 24 h, obvious diffraction peaks of boehmite[18] (JCPDS PDF No. 832384) can be detected (Figure 7d). After a prolonged reaction time of 48 h, increases in the intensities of the XRD peaks are observed (Figure 7e). The aluminum content, measured by ICP, in the supernatant of the first-time centrifugal AU(48) sample is 0.3

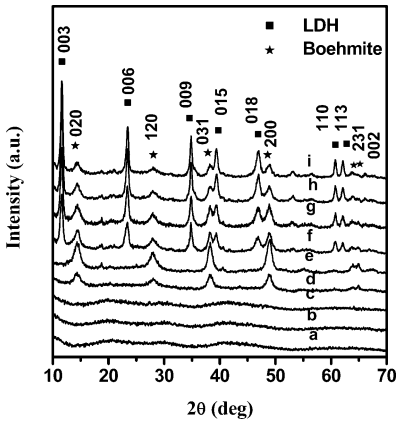

Figure 7. XRD patterns of the samples prepared using only $Al(NO_3)_3{\cdot}9H_2O$ and urea as raw materials, with different reaction times: (a) AU(0), (b) AU(4), (c) AU(8), (d) AU(24), and (e) AU(48). Then, $Mg(NO_3)_2{\cdot}6H_2O$ was added after a reaction time of 48 h, and the samples were obtained after additional reaction times: (f) AU-M(16), (g) AU-M(24), (h) AU-M(48), and (i) AU-M(72).

μg/mL, which is a very minute amount of aluminum compared to the starting aluminum concentration (4.5×10^3 μg/mL), indicating that almost all aluminum ions are converted into the boehmite phase. Then, magnesium nitrate hexahydrate was added to the reaction system with the same concentration ratio of urea/Al/Mg as that of experiment I. It is obvious that LDH diffraction peaks appear after an additional reaction time of 16 h (Figure 7f). Moreover, increasing the reaction time can lead to a gradual increase in the intensity of the LDH phase and a simultaneous progressive decrease of the boehmite phase (Figure 7g−i), demonstrating that the as-formed boehmite phase is transformed into LDH phase.

SEM of Figure 8a shows that when the reaction solution became turbid after mixing a solution of aluminum nitrate nonahydrate and urea for about 6.5 h, there are substantial

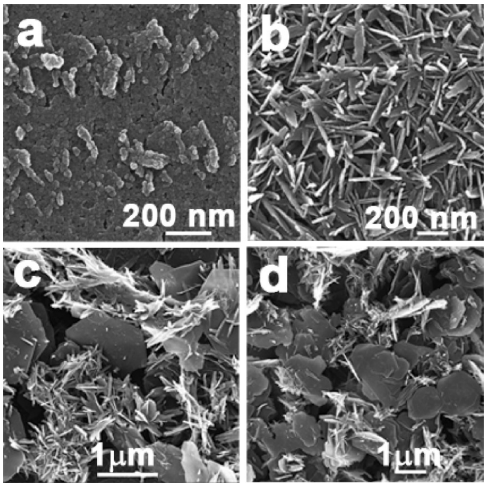

Figure 8. SEM images of samples: (a) AU(0), (b) AU(48), (c) AU-M(24 h), and (d) AU-M(48 h). The sample labels are the same as in Figure 7.

amorphous aggregates in the AU(0) sample. In Figure 8b, boehmite particles with narrow lamellar morphology appear in the AU(48) sample, after a reaction time of 48 h, without adding the magnesium nitrate precursor. After adding

dx.doi.org/10.1021/cm201936b | Chem. Mater. 2012, 24, 81−87

magnesium nitrate, both lamellar boehmite and plate-like LDH crystallites exist (Figure 8c and d). Moreover, the amount of plate-like LDH rises with the reaction time increase. Thus, we conclude that the LDH crystallites are formed through the consuming of the as-formed boehmite.

FT-IR spectra of samples were provided in Figure 9. For the five samples prepared without the addition of magnesium nitrate precursor, an intense adsorption band around 1384

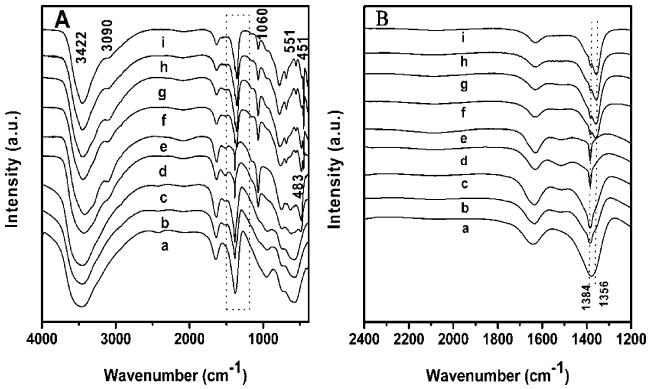

Figure 9. FT-IR spectra of samples (A). (B) the magnifying FT-IR spectra from 1200 cm^{-1} to 2400 cm^{-1}. The sample labels are the same as in Figure 7.

cm^{-1} appears,[16] which is ascribed to the symmetric stretching mode of NO_3^- ions existing in amorphous hydroxide aluminum AU(0), AU(4), AU(8), and boehmite AU(24) and AU(48). What attracts our attention is that the intense band at 1384 cm^{-1} gradually disappears after the addition of magnesium nitrate. Instead, the absorption band of CO_3^{2-} ions at 1356 cm^{-1} presents[16] for the series of AU-M samples, which verifies that NO_3^- ions are progressively replaced by CO_3^{2-} ions.

According to the literature, the formation process of LDH crystallites by coprecipitation can be divided roughly into two stages:[10,11b−d] the first stage corresponds to the formation of aluminum hydroxide or hydrous oxide in the presence of excess Al^{3+}, followed by the formation of LDH from aluminum hydr(ous)oxide in the presence of excess Mg^{2+}. Based on the above evaluation process and the previous findings of other groups, we propose a detailed formation mechanism of LDH structure (Figure 10). At the very beginning of crystallization, because the precipitation pH of Al^{3+} is lower than that of

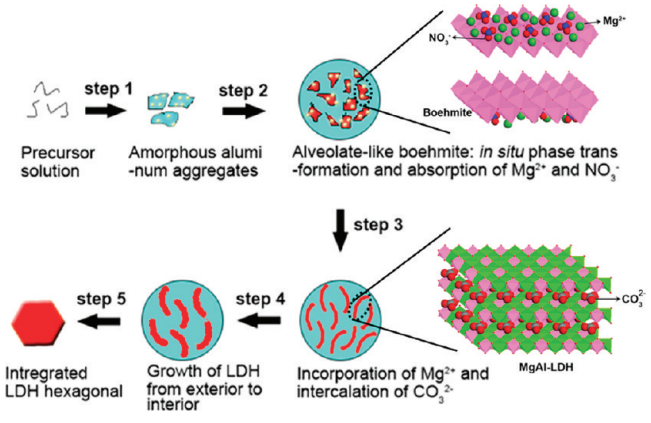

Figure 10. Schematic illustration of a proposed crystal evolution process of LDH.

Mg^{2+},[19] sequential hydrolysis and polycondensation of Al^{3+} and urea kinetically favor the precipitation of amorphous aluminum hydroxide with featureless morphology. Meanwhile, NO_3^- and a small quantity of Mg^{2+} ions are absorbed on the surface (step 1). These aluminum hydroxide particles further gradually collect into sphere-like aggregates. Simultaneously, an *in situ* phase transformation from amorphous aluminum to lamellar boehmite occurs, forming numerous nanoflakes on the surface of the spherical particles and thus leading to an alveolate-like structure (step 2). In this stage, we note that NO_3^- and a larger quantity of Mg^{2+} ions are absorbed on the surface of these alveolate-like particles. In the next step, the incorporation of the surface-absorbed Mg^{2+} into the sheet of the lamellar boehmite occurs subsequently, which leads to the unbalance of the sheet charge and destroys the interlamellar hydrogen bonds; therefore, carbonate ions are intercalated into the interlayer to balance the charge and the stacking of sheets begins to form layered structure (step 3). The literature has reported the crystallization of LDH occurring by means of the diffusing of aluminum atoms into the magnesium hydroxide structure,[11c] while others regard it through the incorporation of magnesium continuously into an Al-rich LDH-type phase.[10,11b,d] The crystallization process has not been thoroughly revealed at present. According to our above systematic investigation, we obtain the direct information to clearly reveal the incorporating of surface-absorbed Mg^{2+} into the sheet of the lamellar boehmite.

It was shown that the abilities of anions to bind with LDH vary considerably, with the affinity decreasing in the order of $CO_3^{2-} > SO_4^{2-} > OH^- > F^- > Cl^- > Br^- > NO_3^-$,[16,20] by comparing their banding energies between the metal hydroxide layers and interlayer anions. The carbonate ion has the largest binding energy among the above inorganic ions; thus, it is the easiest to be intercalated into the gallery between the main layers. As in the coexisting system of nitrate and carbonate ions, nitrate ions are less likely to be intercalated into the interlayer. The pH value of the synthesizing solution is also an important aspect to influence the sort of the charge balancing anion in the LDH interlayer space. In the literature, the synthesis of ZnAl-LDHs, with nitrate as the interlayer anion under low pH value, also with short reaction time or high NO_3^-/urea molar ratio, using the urea method, was reported.[21] There were also reports in the literature that, at the very beginning of the reaction for ZnAl-LDHs system, zinc specimens containing the final intercalated anions for LDHs were formed first, rather than aluminum hydroxide.[12b,22] This was opposite to the MgAl-LDH system, through which, usually, only carbonate containing MgAl-LDH could be synthesized by this method.[5a−c,23] This discrepancy is acceptable if we agree with the concept expressed by Walter[24] that each LDH material requires its own procedure to be obtained in the best way. Hitherto, the multiple nucleation of LDH has been achieved on the surface, generating crystalline particles. These small crystalline particles extend on the spherical surface, fuse together, and adjust their orientations, thus forming hexagonal plate-like LDH. The crystallization and growth of LDH crystallites occurs from the exterior to the interior of the aggregates (step 4), and finally, an integrated and perfect hexagonal LDH is formed (step 5).

In short, the entire evolution process is the result of urea hydrolysis, precipitation of aluminum hydroxide, phase transformation of amorphous aluminum hydroxide, incorporation of magnesium ions, intercalation of carbonate ions, stacking of the sheets, and the growth by repining of LDH. Among the above-

dx.doi.org/10.1021/cm201936b | *Chem. Mater.* 2012, 24, 81−87

mentioned processes, the incorporation of magnesium ions into the sheet of the lamellar boehmite can play a primary role for the formation of LDH crystallites.

CONCLUSIONS

In summary, we systematically investigate the evolution process of the LDH formed by coprecipitation with aqueous solution of aluminum salts, magnesium salts, and urea. The as-synthesized samples are characterized by using HRTEM combined with SAED, FESEM, XRD, FT-IR, and XPS measurements. A five-step evolution process is proposed according to the whole experimental results associated with the previous findings of other groups, which is the result of urea hydrolysis, precipitation of aluminum hydroxide, phase transformation of amorphous aluminum hydroxide, incorporation of magnesium ions, intercalation of carbonate ions, stacking of the sheets, and the growth by repining of LDH. It is worthy noting that we obtain the direct information to clearly reveal the incorporating of the surface-absorbed Mg^{2+} into the sheet of the lamellar boehmite and the subsequent stacking of layers into LDH phase. We hope that this process strategy could favor a further understanding and insight on the synthetic methodologies of LDH materials.

ASSOCIATED CONTENT

Supporting Information

SEM images of more particles in sample LDH(4). This material is available free of charge via the Internet at http://pubs.acs.org.

AUTHOR INFORMATION

Corresponding Author

*Tel: (+86) 10-6442-5105. Fax: (+86) 10-6442-5385. E-mail: zhangfz@mail.buct.edu.cn.

ACKNOWLEDGMENTS

This work was financially supported by the National Natural Science Foundation of China and the 973 Program (No. 2011CBA00506).

REFERENCES

(1) (a) Williams, G. R.; O'Hare, D. *J. Mater. Chem.* **2006**, *16*, 3065–3074. (b) Evans, D. G.; Duan, X. *Chem. Commun.* **2006**, *6*, 485–496. (c) Auerbach, S. M.; Carrado, K. A.; Dutta, P. K., *Handbook of Layered Materials*; Marcel Dekker. Inc: New York, 2004; (d) Rives, V.; Angeles Ulibarri, M. *Coord. Chem. Rev.* **1999**, *181*, 61–120. (e) Cavani, F.; Trifirò, F.; Vaccari, A. *Catal. Today* **1991**, *11*, 173–301.

(2) Evans, D. G.; Slade, R. C. T. *Struct. Bonding (Berlin)* **2006**, *119*, 1–87.

(3) (a) Zhang, F. Z.; Xiang, X.; Li, F.; Duan, X. *Catal. Surv. Asia* **2008**, *12*, 253–265. (b) Taviot-Guého, C.; Leroux, F. *Struct. Bonding (Berlin)* **2006**, *119*, 121–159. (c) Li, F.; Duan, X. *Struct. Bonding (Berlin)* **2006**, *119*, 193–223. (d) Tichit, D.; Coq, B. *CATTECH* **2003**, *7*, 206–217. (e) Sels, B. F.; De Vos, D. E.; Jacobs, P. A. *Catal. Rev. Sci. Eng.* **2001**, *43*, 443–488. (f) Costantino, U.; Ambrogi, V.; Nocchetti, M.; Perioli, L. *Microporous Mesoporous Mater.* **2008**, *107*, 149–160. (g) Hwang, S. H.; Han, Y. S.; Choy, J. H. *Bull. Korean Chem. Soc.* **2001**, *22*, 1019–1022. (h) Costantino, U.; Casciola, M.; Massinelli, L.; Nocchetti, M.; Vivani, R. *Solid State Ionics* **1997**, *97*, 203–212. (i) Chen, T.; Xu, S. L.; Zhang, F. Z.; Evans, D. G.; Duan, X. *Chem. Eng. Sci.* **2009**, *64*, 4350–4357.

(4) (a) Shylesh, S.; Schünemann, V.; Thiel, W. R. *Angew. Chem., Int. Ed.* **2010**, *49*, 3428–3459. (b) Yin, Y.; Alivisatos, A. P. *Nature* **2005**, *437*, 664–70. (c) Sun, Y.; Xia, Y. *Science* **2002**, *298*, 2176–2179.

(5) (a) Adachi-Pagano, M.; Forano, C.; Besse, J.-P. *J. Mater. Chem.* **2003**, *13*, 1988–1993. (b) Ogawa, M.; Kaiho, H. *Langmuir* **2002**, *18*, 4240–4242. (c) Costantino, U.; Marmottini, F.; Nocchetti, M.; Vivani, R. *Eur. J. Inorg. Chem.* **1998**, *1998*, 1439–1446. (d) Okamoto, K.; Iyi, N.; Sasaki, T. *Appl. Clay Sci.* **2007**, *37*, 23–31.

(6) Xu, Z. P.; Stevenson, G. S.; Lu, C. Q.; Lu, G. Q.; Bartlett, P. F.; Gray, P. P. *J. Am. Chem. Soc.* **2006**, *128*, 36–37.

(7) Zhao, Y.; Li, F.; Zhang, R.; Evans, D. G.; Duan, X. *Chem. Mater.* **2002**, *14*, 4286–4291.

(8) Abelló, S.; Pérez-Ramírez, J. *Adv. Mater.* **2006**, *18*, 2436–2439.

(9) Hu, G.; O'Hare, D. *J. Am. Chem. Soc.* **2005**, *127*, 17808–17813.

(10) Seron, A.; Delorme, F. *J. Phys. Chem. Solids* **2008**, *69*, 1088–1090.

(11) (a) Xu, Z. P.; Lu, G. Q. *Chem. Mater.* **2005**, *17*, 1055–1062. (b) Fogg, A. M.; Williams, G. R.; Chester, R.; O'Hare, D. *J. Mater. Chem.* **2004**, *14*, 2369–2371. (c) Eliseev, A. A.; Lukashin, A. V.; Vertegel, A. A.; Tarasov, V. P.; Tret'yakov, Y. D. *Dokl.Chem.* **2002**, *387*, 339–343. (d) Boclair, J. W.; Braterman, P. S. *Chem. Mater.* **1999**, *11*, 298–302.

(12) (a) Oh, J. M.; Hwang, S. H.; Choy, J. H. *Solid State Ionics* **2002**, *151*, 285–291. (b) Benito, P.; Herrero, M.; Barriga, C.; Labajos, F. M.; Rives, V. *Inorg. Chem.* **2008**, *47*, 5453–5463.

(13) (a) Machida, M.; Takenami, M.; Hamada, H. *Solid State Ionics* **2004**, *172*, 125–128. (b) Inoue, M.; Kondo, Y.; Inui, T. *Chem. Lett.* **1986**, *15*, 1421–1424.

(14) (a) Sharma, U.; Tyagi, B.; Jasra, R. V. *Ind. Eng. Chem. Res.* **2008**, *47*, 9588–9595. (b) Kovanda, F.; Kolousek, D.; Cílová, Z.; Hulínský, V. *Appl. Clay Sci.* **2005**, *28*, 101–109.

(15) (a) Villholth, K. G. *Environ. Sci. Technol.* **1999**, *33*, 691–699. (b) Casellato, U.; Cattarin, S.; Guerriero, P.; Musiani, M. M. *Chem. Mater.* **1997**, *9*, 960–966.

(16) Ma, S.; Fan, C.; Du, L.; Huang, G.; Yang, X.; Tang, W.; Makita, Y.; Ooi, K. *Chem. Mater.* **2009**, *21*, 3602–3610.

(17) Ma, S.; Fan, C.; Huang, G.; Li, Y.; Yang, X.; Ooi, K. *Eur. J. Inorg. Chem.* **2010**, *2010*, 2079–2083.

(18) (a) Lepot, N.; Van Bael, M. K.; Van den Rul, H.; D'Haen, J.; Peeters, R.; Franco, D.; Mullens, J. *Ceram. Int.* **2008**, *34*, 1971–1974. (b) Lee, H. W.; Park, B. K.; Tian, M. Y.; Lee, J. M. *J. Ind. Eng. Chem.* **2006**, *12*, 295–300. (c) Hou, H.; Xie, Y.; Yang, Q.; Guo, Q.; Tan, C. *Nanotechnology* **2005**, *16*, 741–745.

(19) Li, B.; He, J.; Evans, D. G. *Chem. Eng. J.* **2008**, *144*, 124–137.

(20) (a) Li, H.; Ma, J.; Evans, D. G.; Zhou, T.; Li, F.; Duan, X. *Chem. Mater.* **2006**, *18*, 4405–4414. (b) Iyi, N.; Matsumoto, T.; Kaneko, Y.; Kitamura, K. *Chem. Mater.* **2004**, *16*, 2926–2932.

(21) Inayat, A.; Klumpp, M.; Schwieger, W. *Appl. Clay Sci.* **2011**, *51*, 452–459.

(22) Chen, H. Y.; Zhang, F. Z.; Chen, T.; Xu, S. L.; Evans, D. G.; Duan, X. *Chem. Eng. Sci.* **2009**, *64*, 2617–2622.

(23) (a) Costa, F. R.; Abdel-Goad, M.; Wagenknecht, U.; Heinrich, G. *Polymer* **2005**, *46*, 4447–4453. (b) Iyi, N.; Matsumoto, T.; Kaneko, Y.; Kitamura, K. *Chem. Mater.* **2004**, *16*, 2926–2932.

(24) Walter, T. R. *Solid State Ionics* **1986**, *22*, 135–141.